Lifetime of surface states on (0001) surfaces of lanthanide metals

A. Bauer, A. Mühlig, D. Wegner, and G. Kaindl
Freie Universität Berlin, Institut für Experimentalphysik, Arnimallee 14, D-14195 Berlin, Germany
(Received 22 March 2001; published 1 February 2002)

We have studied the electronic structure of surface states on (0001) surfaces of Gd, Ho, and Lu films with scanning-tunneling spectroscopy at low temperature (10 K). The $5d_{z^2}$-like surface states have a small dispersion and exhibit magnetic exchange splittings that are proportional to the $4f$-spin moment, being largest for Gd and zero for Lu. The surface state in Lu lies directly at the Fermi energy, resulting in a sharp peak in the tunneling spectrum. A line-shape analysis of the tunneling spectra reveals linewidths and, hence, lifetimes of surface-state electrons governed by electron-phonon and electron-electron scattering.

DOI: 10.1103/PhysRevB.65.075421 PACS number(s): 73.20.At, 73.50.Gr, 71.20.Eh

I. INTRODUCTION

Surfaces of crystals with local bandgaps in the surface Brillouin zone often exhibit surface states that decay exponentially into both the bulk and the vacuum and are thus confined to a thin surface layer. Binding energies and dispersions of surface states have been studied for many materials. More recently, increasing attention has also been given to the lifetimes of these states[1,2] as this is of importance for processes at surfaces where charge transfer is involved (e.g., chemical reactions). However, a profound understanding of surface-state lifetimes is still lacking for most systems.[2] Even for the most extensively studied *sp*-like surface states in noble metals, a quantitative description was not obtained until very recently by Kliewer *et al.*[3]

Electronic structure and lifetimes of surface states have mostly been studied by photoemission (PE) or inverse photoemission (IPE) in the past.[2] The first systematic studies of surface-state lifetimes with scanning-tunneling microscopy (STM) and scanning-tunneling spectroscopy (STS) were performed by Li *et al.*[4] and Bürgi, Jeandupeux, Brune, and Crampin.[5] Advantages of STS over PE or IPE are (i) the comparatively high-energy resolution at low temperatures (a few meV or even less), (ii) the access to states on both sides of the Fermi energy, and (iii) the high-spatial resolution. The latter is of importance if impurities or surface defects disturb the local electronic structure. In this case, it becomes difficult to determine inherent properties of ideal surfaces with spatially averaging techniques.[6] The major drawback of STS is that the exact portion of k space probed by the tunneling electrons is not exactly known and depends strongly on the tip geometry as well as on the electronic band structure of tip and sample.

In this paper, we present tunneling spectra recorded at 10 K on (0001) surfaces of Gd, Ho, and Lu. The $5d_{z^2}$-like surface states (Tamm states) that exist in the closed-packed (0001) surfaces of all trivalent lanthanide metals[7] appear as sharp peaks in the tunneling spectra.[8,9] They are located in local band gaps around the $\bar{\Gamma}$ point.[10,11] Their energy is close to the Fermi energy E_F and they exhibit only small dispersion due to a high degree of localization. Since the $5d_{z^2}$ orbitals extend far into the vacuum, STS is highly sensitive to these states. Due to exchange interaction with the $4f$ electrons the surface states exhibit an exchange splitting that is proportional to the $4f$-spin moment. In general, it results in an occupied state below E_F with the spin parallel to the $4f$ spin (majority spin), and an unoccupied state above E_F with antiparallel spin alignment.[12]

By analyzing the line shape of the surface-state peaks on the basis of simple planar-tunneling theory and by taking into account a small dispersion of the surface states, we have determined the linewidths, i.e., inverse lifetimes, of surface states in Gd, Ho, and Lu. Since the band structure of the lanthanide metals is similar, the observed binding-energy dependence of the surface-state lifetime can, to first approximation, be attributed to the energy dependence of electron-electron scattering, which had not yet been studied for the lanthanides, neither experimentally nor theoretically.

II. EXPERIMENTAL DETAILS

The experiments were performed in a UHV system that is equipped with a low-temperature STM and sample-preparation facilities. The base pressure in the UHV system is typically 5×10^{-11} mbar. The STM consists of a commercial STM head (Omicron) mounted into a home-built liquid-helium-bath cryostat. The transferable STM head is placed inside a copper cage that is cooled by He-exchange gas within two bellows by which the cage is suspended to provide vibration isolation. The measurements presented here were performed at (10 ± 0.5) K (measured on the sample holder). The preamplifier for the tunneling current is located outside the UHV chamber, and the STM/STS measurements are controlled by a digital signal processor.

For STS measurements, the tunneling current I and the differential conductivity dI/dU are recorded as a function of sample bias U at fixed STM-tip position. Close to E_F, the latter is in good approximation proportional to the local density of states of the sample at an energy $E-E_F=eU$. We measure the conductivity by modulating the bias voltage ($f_{\mathrm{mod}}\approx300$ Hz, $\Delta U^{\mathrm{rms}}\approx1$ mV) and detecting the amplitude of the tunneling-current modulation with a lock-in amplifier.

The (0001)-lanthanide films are deposited at room temperature on clean W(110) surfaces by electron-beam evapo-

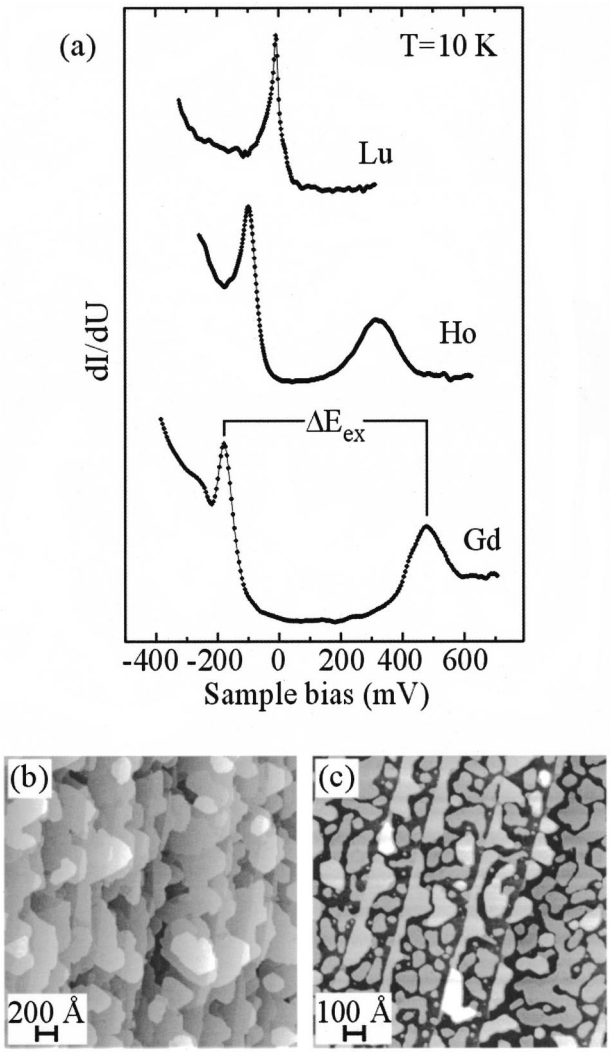

FIG. 1. (a) Representative tunneling spectra recorded on different lanthanide-metal films at 10 K. (b,c) STM images of (b) a 2-ML and (c) a 14-ML thick Ho/W(110) film. Both films were annealed under same conditions at a temperature less than 700 K. The thin film is broken up into (2–3)-ML high islands with atomically flat surfaces, sitting on top of a continuous Ho monolayer. The thick film is continuous and was smoothed upon annealing (it would need higher temperatures to break it up). STM images of Gd/W(110) films look very similar.

ration out of a Ta crucible. The film thickness is controlled by a quartz microbalance with an error of about ±20%. After deposition the films were annealed at temperatures up to 1000 K. The quality of the films is checked by low-energy electron diffraction (LEED) and STM. The W(110) single crystal is clamped by small wedges into a transferable sample holder. All parts are made of tungsten. In this way, the W(110) crystal can be annealed at temperatures above 2300 K using a specially designed electron-beam heating stage. This is necessary to prepare clean surfaces and to remove tungsten oxides from the surface, especially after the crystal was annealed in oxygen (2×10^{-8} mbar) in order to remove carbon contamination from the surface.

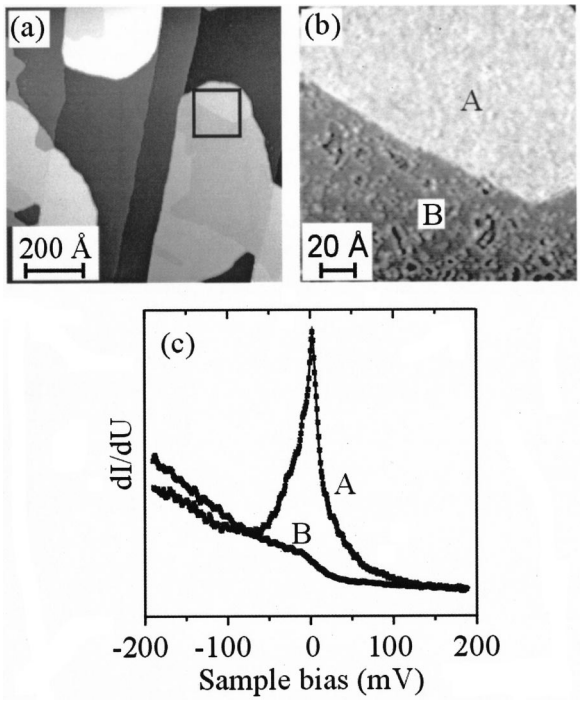

FIG. 2. (a) STM image of 3 ML Lu/W(110) after annealing at 1000 K. Image (b) is a magnification of the marked area in (a). (c) Tunneling spectra taken on Lu islands of this film in morphologically different surface regions, *A* and *B*, indicated in image (b). Region *B* is obviously contaminated (possibly by oxygen), resulting in a suppression of the surface state.

III. RESULTS AND DISCUSSION

In Fig. 1(a), we show dI/dU spectra measured on (0001) surfaces of Gd, Ho, and Lu films. The exchange-split surface states appear as pronounced peaks in the spectra with the largest exchange splitting observed for Gd and zero splitting for Lu. The spectra were recorded on atomically flat surfaces of either continuous films or three-dimensional islands with a thickness greater and equal to 3 monolayers (ML) and areas of at least 100 nm^2. Due to large effective masses of the surface states ($m^*/m>5$, see below), the impact of lateral confinement on the surface states should be negligible for these dimensions.[13] The islands were produced by annealing (2–3)-ML thick films (at temperature up to 1000 K) as seen in Fig. 1(c).[14] Continuous films were obtained for larger thicknesses upon annealing [see Fig. 1(b)]. LEED showed a sharp hexagonal (1×1) pattern and, for the island films, the expected superstructure from the first monolayer on W(110).[14,15] While the surfaces of Gd and Ho films were almost free of contamination, it was rather difficult to prepare clean Lu films. We always observed two coexisting phases on Lu-film surfaces [see Fig. 2(a, b)]. In one phase, the surface state at E_F is suppressed [spectrum *B* in Fig. 2(c)] and we observe some scattered holes in the surface, possibly due to oxygen contamination. The other phase exhibits a surface state [spectrum *A* in Fig. 2(c)]. However, the surface morphology is not as atomically flat as found for Gd and Ho surfaces, and impurity-scattering effects cannot be excluded.

It should be mentioned that for thicknesses between 3 and

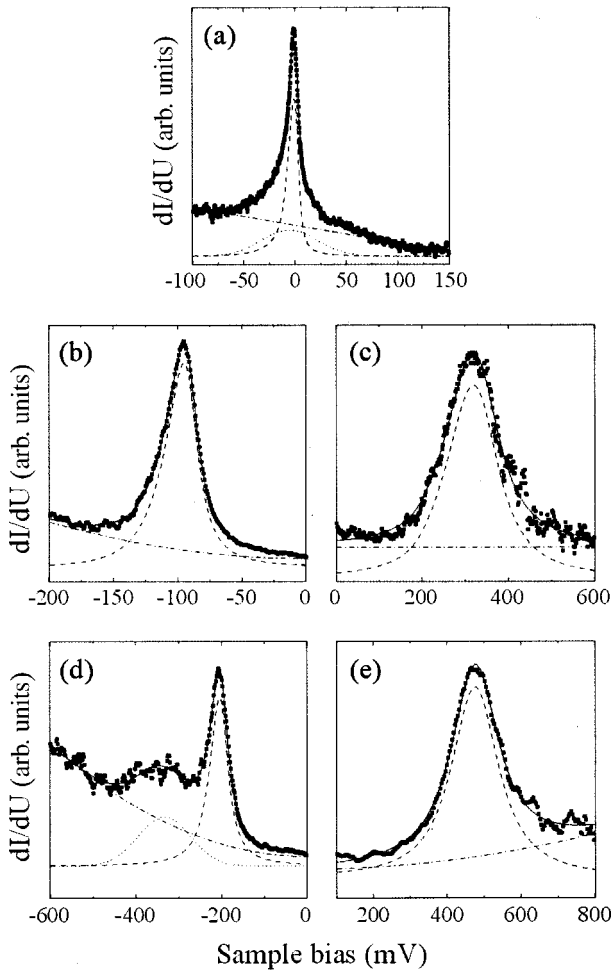

FIG. 3. High-resolved tunneling spectra taken on (a) Lu, (b,c) Ho, and (d,e) Gd films at 10 K. Solid lines: Least-squares fits to the experimental data composed of three subspectra: a surface-state line (dashed), a Gaussian function (dotted), and a linear or quadratic background (dash dotted). The latter is attributed to tunneling into bulk states. Fit parameters are listed in Table I.

14 ML, we did not observe any thickness dependence of the tunneling spectra. Therefore, we assume that the spectra we present here are representative for surfaces of lanthanide-bulk material. It is not yet understood why the exchange splitting is apparently not affected by finite-size effects as could be anticipated from the well-known thickness dependence of the Curie temperature previously measured for Gd films.[16] At higher temperature ($T=67$ K), Bode *et al.* found indeed reduced exchange splittings for less than 4-ML thick Gd islands.[8] A detailed discussion of the temperature and thickness dependence of the exchange splitting will be given in a forthcoming publication.[17]

For a quantitative analysis of the spectral shape of the surface states, we have measured high-resolution spectra for each peak (see Fig. 3). The observed asymmetry in the Lu peak indicates that dispersion of the surface states, although it is rather small in lanthanides,[7,10,11] cannot be fully neglected (i.e., also states with $k_\parallel \neq 0$ contribute to the tunneling current). To first approximation, we assume a quadratic dispersion with negative effective mass, $m^*<0$: $E(k_\parallel)=E_0+(\hbar^2/2m^*)k_\parallel^2$ with E_0 the energy of the surface state (relative to E_F) at the $\bar{\Gamma}$ point, and $k_\parallel$ the parallel momentum. In a simple model of planar tunneling, the tunneling current is given by $I \propto \int_{-\infty}^{\infty} n_T(E-eU) n_S(E) T(E,U)[f(E-eU)-f(E)]dE$, where T is the transmission coefficient for tunneling, n_T and n_S are the density of states of tip and sample, respectively, and f is the Fermi-distribution function.[18] Assuming that the bias dependence of T can be neglected for small U, and that the density of states in the tip is constant (within the energy range of interest), the differential conductivity is

$$\frac{dI}{dU} \propto p_0 \int_{-\infty}^{\infty} dE (n_s T)(E) f'(E-eU), \tag{1}$$

with f' the derivative of f and p_0 a proportionality factor. For a two-dimensional surface-state band with $m^*<0$, the density of states is a step function, $n_S = n_0 \theta(E_0-E)$, and the transmission coefficient is given by

$$T = \exp[-2\sqrt{(2m/\hbar^2)(\phi_{\text{eff}}-E_\perp)}d]$$

with ϕ_{eff} the effective work function, $E_\perp$ the perpendicular energy component, and d the barrier width. For $|m^*| \gg m$, $E_\perp$ can be expressed as

$$E_\perp = (m^*/m)E_0 + [1-(m^*/m)]E \approx (m^*/m)(E_0-E).$$

For $E_\perp < \phi_{\text{eff}}$, the transmission coefficient can thus be approximated by

$$T \propto \exp[-p_1(E_0-E)] \quad \text{with} \quad p_1 = \sqrt{(2m/\hbar^2\phi_{\text{eff}})}(-m^*/m)d. \tag{2}$$

A large p_1 factor is responsible for the appearance of rather narrow peaks in the spectra. In comparison, *sp*-like surface states exhibit generally much smaller effective masses, and thus smaller p_1 values, which leads to step-function-like features in the tunneling spectra.[3,4]

To take into account finite lifetimes of the surface states τ, the function $(n_s T)(E)$ in Eq. (1) is written as an integral over Lorentian functions weighted with the transmission factor T,

$$(n_s T)(E) \propto \int d\varepsilon \frac{\Gamma(\varepsilon)}{(E-\varepsilon)^2 + \frac{1}{4}\Gamma^2(\varepsilon)} \theta(E_0-\varepsilon) \times \exp[-p_1(E_0-\varepsilon)]. \tag{3}$$

The width of the Lorentian function (full width at half maximum) Γ is related to τ by $\tau = \hbar/\Gamma$. Two contributions to the lifetime broadening of the surface state are considered here: electron-phonon (e-ph) scattering ($\Gamma_{e\text{-ph}} = \hbar/\tau_{e\text{-ph}}$) and electron-electron (e-e) scattering ($\Gamma_{e\text{-}e} = \hbar/\tau_{e\text{-}e}$).

At zero temperature, within the Debye model, $\Gamma_{e\text{-ph}}$ is given by[19,20]

TABLE I. Average values for E_0, ΔE_{ex}, p_1, β, Γ, and τ obtained from fits of tunneling spectra such as the ones shown in Fig. 3, as well as measured Debye frequencies ω_D and calculated electron-phonon mass-enhancement factors λ taken from the literature for Lu, Ho, and Gd.[23] Line widths due to *e*-ph scattering, $\Gamma_{e\text{-ph}}(E_0)$, were calculated with Eq. (4). The fit parameters varied for different sets of spectra by about 5% for E_0, 10% for β, $\Gamma(E_0)$, and $\tau(E_0)$, and up to 40% for p_1 (see text). The surface-state lifetimes τ were calculated from $\tau=\hbar/\Gamma$.

$4f$ metal	E_0 (meV)	ΔE_{ex} (meV)	p_1 (eV^{-1})	β (eV^{-1})	$\Gamma(E_0)$ (meV)	$\tau(E_0)$ (fs)	λ [23]	$\hbar\omega_D$ (meV)	$\Gamma_{e\text{-ph}}(E_0)$ (meV)
Lu	2.3		128		5.2	127	0.59	15.8 (Ref. 22)	0.05
Ho	−90	437	89	0.52	19	35	0.30	16.4 (Ref. 21)	10.3
	347		32	0.48	125	5.3			
Gd	−182	673	89	0.50	44	15	0.40	14.0 (Ref. 22)	11.7
	491		55	0.25	132	5.0			

$$\Gamma_{e\text{-ph}}(T=0)=\begin{cases}\dfrac{2\pi}{3}\lambda\dfrac{|E-E_F|^3}{(\hbar\omega_D)^2}, & |E-E_F|<\hbar\omega_D,\\ \dfrac{2\pi}{3}\lambda\hbar\omega_D, & |E-E_F|\geq\hbar\omega_D,\end{cases} \tag{4}$$

with ω_D the Debye frequency and λ the electron-phonon mass-enhancement factor. The increase of $\Gamma_{e\text{-ph}}$ from $T=0$ to $T=10$ K is small[19,20] (<1 meV) and can be neglected here. For our fits, we used measured ω_D values[21,22] and calculated λ values[23] listed in Table I. It should be noted that these values describe bulk properties, and that for the surface, ω_D and λ may differ from the bulk values. However, changes are expected to be less than 10%, as was recently demonstrated by calculations for noble metals.[3]

The $(e\text{-}e)$-scattering contribution to the linewidth $\Gamma_{e\text{-}e}$ is given by Fermi-liquid theory,[20,24]

$$\Gamma_{e\text{-}e}=2\beta[(\pi k_B T)^2+(E-E_F)^2]. \tag{5}$$

Since the factor β is of the order of 1 eV^{-1}, the first term in Eq. (5) can be ignored here. In cases where the binding energy $E-E_F$ amounts to only a few meV (such as for Lu), the second term also becomes small and $\Gamma_{e\text{-}e}$ is thus negligible ($\Gamma_{e\text{-}e}\ll 1$ meV).

In summary, the surface-state peaks were fitted according to Eqs. (1)–(5) with four parameters, E_0, β, p_0, and p_1, used as fit parameters. The temperature that enters the Fermi-distribution function was set to 10 K. For zero binding energy ($E-E_F=0$), the model predicts vanishing linewidths due to *e-e* and *e*-ph scattering. In the ideal experiment, spectral broadening by about $3.5k_BT\approx 3$ meV (at $T=10$ K) would be expected from the convolution with the derivative of the Fermi-distribution function in Eq. (1). Experimentally, however, we find broader structures at small binding energies in the Lu spectra [$E_0(\mathrm{Lu})\approx 2$ meV, see below]. The reason for this additional broadening is not yet fully understood. It might be an experimental artifact, e.g., due to rf-noise pick-up on the sample bias. Such effects could be accounted for by convoluting the spectra with a Gaussian function, which, however, did not result in good fits. Better fits were obtained by increasing the Lorentian linewidth. This could possibly be caused by defect scattering due to structural disorder at the surface of Lu films, which was observed by STM. Therefore, for Lu, we added as further fit parameter an energy independent offset to the Lorentian linewidth.

In Fig. 3, we show least-squares fits of the tunneling spectra for Lu, Ho, and Gd. The calculated spectra are composed of three components: (i) the surface-state peak according to the model described above, (ii) a linear or quadratic background attributed to bulk-state contributions, and (iii) a Gaussian line to account for some extra features in the spectra (see discussion below). As is seen in Fig. 3, the experimental data is fairly well reproduced by the fits. The obtained values for p_1, E_0, β, and its corresponding values, $\Gamma(E_0)$ and $\tau(E_0)$, as well as ΔE_{ex} are listed in Table I. The p_1 values, which are proportional to m^*, are of the same order of magnitude. Since the parameters ϕ_{eff} and d are not exactly known [see definition of p_1 in Eq. (2)], however, an accurate determination of m^* is not possible. Nevertheless, by assuming $\phi_{eff}\geq 2$ eV and $d\leq 15$ Å, we can estimate $m^*/m>5$, that underlines the high degree of localization of the surface states. For different spectra, p_1 varies up to 40%. Certainly, it does not originate from different dispersions. We assume that a different angular distribution in the tunneling process is responsible for this variation, e.g., due to different tip geometries or surface inhomogeneities. However, this has only weak influence on the other parameters. The variation of E_0 and Γ for different spectra is less than 5% and 11%, respectively.

As mentioned before, additional features are observed in some tunneling spectra such as the peak to the left of the occupied Gd surface-state peak in Fig. 3(d). They can most likely be attributed to tip states since they were not reproducible for different tips. The Gaussian line added to the fit of the Lu spectrum [dotted line in Fig. 3(a)], however, might have a different origin and is not necessarily a tip-induced feature, as the broad tails have been observed in all spectra. The applied model might be too simple to allow for a quantitative description of the full spectrum. On the one hand, the pronounced peak close to the Fermi energy (zero bias) can only be fitted by assuming a high effective mass, i.e., a rather narrow binding-energy range (~7 meV below E_0) that contributes to the surface-state peak. On the other hand, a fit of the broader structures (tails) in the spectrum would require a much wider energy range to give contributions to the spectral shape, i.e., a smaller effective mass. It could be a hint that

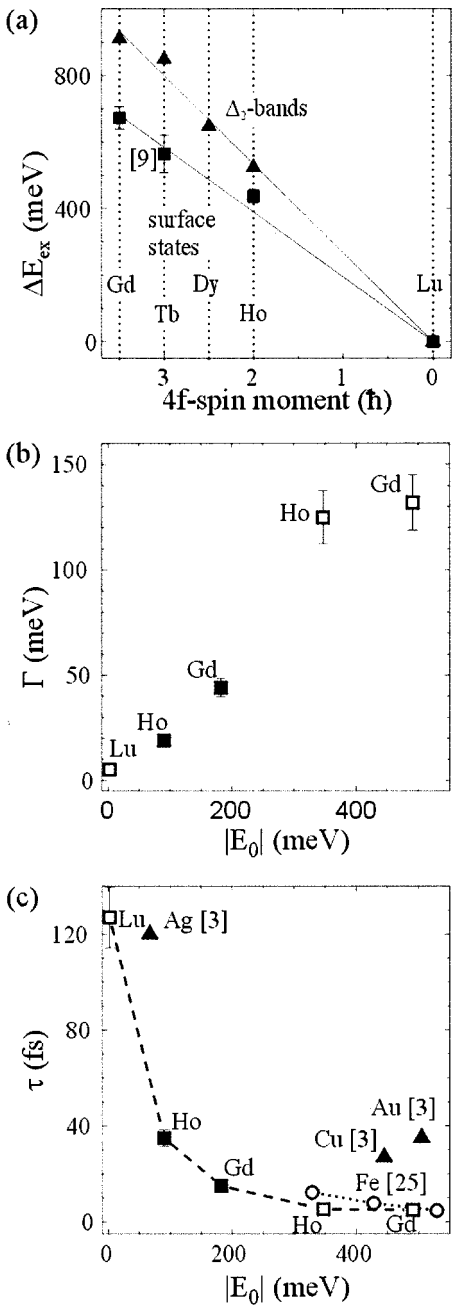

FIG. 4. (a) Exchange splitting of surface states (squares) vs $4f$-spin moment. The data point for Tb was obtained with STS by Bode *et al.*[9] For comparison, we have also plotted data points for bulk states (exchange splitting of Δ_2 bands at the Γ point in the Brillouin zone) obtained by photoelectron spectroscopy (triangles) (Ref. 26). The solid lines represent linear fits to the data with slopes of (268 ± 16) meV (Ref. 26) and (195 ± 9) meV for bulk and surface states, respectively. (b) Linewidths, Γ, and (c) corresponding surface-state lifetimes, $\tau=\hbar/\Gamma$ (squares), as a function of absolute value of binding energy, $|E_0|$. In (c), for comparison, we have plotted lifetimes of *sp*-like surface states on (111) surfaces of noble metals (Cu, Ag, Au) obtained[3] by STS as well as lifetimes of valence-band states (bulk states) in Fe obtained by time-resolved two-photon photoemission (Ref. 25). Filled (open) symbols in (b,c) represent lifetimes of states below (above) E_F.

the effective mass is energy dependent, however, a more elaborate theory is needed here for a quantitative description.

In Fig. 4(a), the exchange splitting $\Delta E_{\rm ex}$, is plotted versus the $4f$-spin moment of the lanthanide atoms. For comparison, we also plotted the exchange splittings of the Δ_2 bands in the bulk that were recently measured by photoelectron spectroscopy.[26] As expected,[27,28] both the surface-state and the bulk-band splittings are proportional to the $4f$-spin moment, however, with different proportionality factors (i.e., effective exchange-coupling constants) for surface and bulk states. A detailed discussion of exchange splittings and their dependence on temperature and film thickness will be published elsewhere.[17]

We shall now discuss the dependence of Γ on the binding energy of the surface-state band maximum E_0 that is presented in Fig. 4(b). The corresponding lifetimes τ are plotted in Fig. 4(c). Since the β factors do not vary by more than a factor of 2 for majority- and minority-spin states nor for different materials (Gd, Ho) (see Table I) we observe an increase of Γ with increasing $|E_0|$. The variation of the β factors is most likely explained by the differences in the spin-dependent band structures of Gd and Ho. The smallest value of Γ is observed for Lu where the surface state is located directly at the Fermi energy (β cannot be determined here since $\Gamma_{e\text{-}e}$ is negligible for binding energies of a few meV). It amounts to $\Gamma(E_0(\mathrm{Lu}))=5.2$ meV. However, as mentioned before, according to Eqs. (4,5) the linewidth should be even smaller (<1 meV) at $E_0(\mathrm{Lu})=2.3$ meV. Whether this enhanced value reflects the experimental energy-resolution limit, or there is indeed an enhanced scattering probability that cannot conclusively be answered at present (see discussion above).

For comparison of our present data with available low-temperature lifetime data, we have plotted in Fig. 4(c) lifetimes of Shockley-type (*sp*-like) surface states in noble metals[3] and of valence-band states in Fe.[25] While the lifetimes of the noble-metal surface states are significantly larger, the lifetimes of Fe-bulk states are comparable to those of the lanthanide-metal surface states. Qualitatively, this can be explained by the different densities of states at the Fermi energy for noble metals (Au, Ag, Cu), on the one hand, and $3d$- or $4f$-transition metals with the strong *d*-band contribution at E_F, on the other hand. The density of states of the $3d$- and $4f$-transition metals is about an order of magnitude larger than that of the noble metals, resulting in an enhanced number of decay channels for hot electrons or holes. This would explain why the β factors for the lanthanide-metal surface states are about an order of magnitude larger than those for surface and bulk states of noble metals (for surface states, Bürgi *et al.*[5] have obtained $\beta=0.019$ eV^{-1} for Cu and $\beta=0.032$ eV^{-1} for Ag).

A quantitative understanding of electron-electron scattering rates for majority-spin and minority-spin states in lanthanide metals would require calculations based on the actual spin-dependent band structure, which have not yet been performed, neither for bulk nor for surface states. It can be expected, however, that the lifetimes of surface and bulk states (at same binding energy) are comparable: Although the $5d_{z^2}$-like surface states are highly localized (in all three di-

mensions) their spatial extension is still of the order of the atomic diameter (unlike, e.g., the much stronger localized $4f$ states).[29] According to calculations by Zarate, Apell, and Echenique,[30] for this degree of localization, lifetimes should not be significantly enhanced with respect to those of delocalized three-dimensional states. This would explain why the lifetimes of the lanthanide surface states are of the same order as those of Fe-bulk states, with both materials having comparable density of states at the Fermi energy.

It is interesting to note that for the noble metals, the lifetimes of surface states are even significantly reduced compared to those of bulk states.[3] This was quantitatively explained by a strong contribution of two-dimensional intraband transitions within the surface-state band.[3] For lanthanide surface states, on the other hand, such intraband transitions are unlikely to occur since, as mentioned, these states are localized not only in one dimension (as for the *sp*-like states) but in all three dimensions, with little overlap. For a quantitative understanding, however, theoretical studies are needed.

IV. SUMMARY

With the present paper, we have gained important information on the electronic structure and dynamics of highly localized states in lanthanide metals. We have measured binding energies and linewidths (i.e., inverse lifetimes) of the exchange-split surface states on (0001) surfaces of thin lanthanide-metal films by low-temperature STS. The exchange splitting is found to be proportional to the $4f$-spin moment with a slope of (195 ± 9) meV. The lifetimes are relatively short and of the same order as those of bulk states of $3d$ transition metals at same binding energy. For the electron-electron scattering contribution, the β factor varied from 0.25 to 0.52 eV^{-1} for the majority- and minority-spin states of Ho and Gd.

ACKNOWLEDGMENT

This work was supported by the Sonderforschungsbereich 290, TPA06 of the Deutsche Forschungsgemeinschaft.

[1] P. M. Echenique, J. M. Pitarke, E. V. Chulkov, and A. Rubio, Chem. Phys. **251**, 1 (2000).
[2] A. Goldmann, R. Matzdorf, and F. Theilmann, Surf. Sci. **414**, L932 (1998).
[3] J. Kliewer, R. Berndt, E. V. Chulkov, V. M. Silkin, P. M. Echenique, and S. Crampin, Science **288**, 1399 (2000).
[4] J. Li, W.-D. Schneider, R. Berndt, O. R. Bryant, and S. Crampin, Phys. Rev. Lett. **81**, 4464 (1998).
[5] L. Bürgi, O. Jeandupeux, H. Brune, and K. Kern, Phys. Rev. Lett. **82**, 4516 (1999).
[6] F. Theilmann, R. Matzdorf, G. Meister, and A. Goldmann, Phys. Rev. B **56**, 3632 (1997).
[7] G. Kaindl, A. Höhr, E. Weschke, S. Vandré, C. Schüssler-Langeheine, and C. Laubschat, Phys. Rev. B **51**, 7920 (1995).
[8] M. Bode, M. Getzlaff, S. Heinze, R. Pascal, and R. Wiesendanger, Appl. Phys. A: Mater. Sci. Process. **A66**, S121 (1998).
[9] M. Bode, M. Getzlaff, A. Kubetzka, R. Pascal, O. Pietzsch, and R. Wiesendanger, Phys. Rev. Lett. **83**, 3017 (1999).
[10] D. Li, C. W. Hutchings, P. A. Dowben, C. Hwang, R. T. Wu, M. Onellion, A. B. Andrews, and J. L. Erskine, J. Magn. Magn. Mater. **99**, 85 (1991).
[11] R. Wu, C. Li, A. J. Freeman, and C. L. Fu, Phys. Rev. B **44**, 9400 (1991).
[12] D. Li, J. Pearson, S. D. Bader, D. N. McIlroy, C. Waldfried, and P. A. Dowben, Phys. Rev. B **51**, 13 895 (1995).
[13] J. Li, W.-D. Schneider, R. Berndt, and S. Crampin, Phys. Rev. Lett. **80**, 3332 (1998).
[14] E. D. Tober, R. X. Ynzunza, C. Westphal, and C. S. Fadley, Phys. Rev. B **53**, 5444 (1996).
[15] S. A. Nepijko, M. Getzlaff, R. Pascal, Ch. Zarnitz, M. Bode, and R. Wiesendanger, Surf. Sci. **466**, 89 (2000).
[16] M. Farle, K. Baberschke, U. Stetter, A. Aspelmeier, and F. Gerhardter, Phys. Rev. B **47**, 11 571 (1993).
[17] A. Bauer, O. Wegner, A. Rehbein, A. Mühlig, and G. Kaindl, J. Electron. Spectrosc. Relat. Phenom. (to be published).
[18] E. L. Wolf, *Principles of Electron Tunneling Spectroscopy* (Oxford, New York, 1985).
[19] G. Grimvall, *The Electron-Phonon Interaction in Metals* (North-Holland, New York, 1981).
[20] B. A. McDougall, T. Balasubramanian, and E. Jensen, Phys. Rev. B **51**, 13 891 (1995).
[21] R. W. Hill, J. Cosier, and D. A. Hukin, J. Phys. F: Met. Phys. **6**, 1731 (1976).
[22] T.-W. E. Tsang, K. A. Gschneider, Jr., F. A. Schmidt, and D. K. Thome, Phys. Rev. B **31**, 235 (1985).
[23] H. L. Skiver and I. Mertig, Phys. Rev. B **41**, 6553 (1990).
[24] J. J. Quinn, Phys. Rev. **112**, 812 (1958); **126**, 1453 (1962).
[25] R. Knorren, K. H. Bennemann, R. Burgermeister, and M. Aeschlimann, Phys. Rev. B **61**, 9427 (2000).
[26] C. Schüßler-Langeheine, E. Weschke, Chandan Mazumdar, R. Meier, A. Yu. Grigoriev, G. Kaindl, C. Sutter, D. Abernathy, G. Grübel, and M. Richter, Phys. Rev. Lett. **84**, 5624 (2000).
[27] C. Schüßler-Langeheine, H. Ott, A. Yu. Grigoriev, A. Möller, R. Meier, Z. Hu, C. Mazumdar, G. Kaindl, and E. Weschke, Phys. Rev. B (to be published).
[28] R. Ahuja, S. Auluck, B. Johansson, and M. S. S. Brooks, Phys. Rev. B **50**, 5147 (1994).
[29] A. J. Freeman, in *Magnetic Properties of Rare Earth Metals*, edited by R. J. Elliot (Plenum, London, 1972).
[30] E. Zarate, P. Apell, and P. M. Echenique, Solid State Commun. **113**, 465 (2000).